Cell Analysis

1

Edited by NICHOLAS CATSIMPOOLAS

Cell Analysis

Volume 1

Edited by
NICHOLAS CATSIMPOOLAS
Boston University School of Medicine
Boston, Massachusetts

PLENUM PRESS • NEW YORK AND LONDON

Library of Congress Cataloging in Publication Data

Main entry under title:

Cell analysis.

Bibliography: p.
Includes index.
1. Cytology—Technique. 2. Cells—Analysis. I. Catsimpoolas, Nicholas. [DNLM: 1. Cells—Analysis—Periodical. W1 CE126H]
QH585.C44 574.87'028 82-5289
ISBN 0-306-40864-3 (v. 1) AACR2

©1982 Plenum Press, New York
A Division of Plenum Publishing Corporation
233 Spring Street, New York, N.Y. 10013

All rights reserved

No part of this book may be reproduced, stored in a retrieval system, or transmitted in any form or by any means, electronic, mechanical, photocopying, microfilming, recording, or otherwise, without written permission from the Publisher

Printed in the United States of America

Contributors

R. B. Allan, *Department of Cell Biology, University of Glasgow, Glasgow G12 8QQ, U.K.*

James W. Bacus, *Medical Automation Research Unit, Rush–Presbyterian–St. Luke's Medical Center, Chicago, Illinois 60612*

S. A. Ben-Sasson, *The Hubert H. Humphrey Centre for Experimental Medicine and Cancer Research, The Hebrew University–Hadassah Medical School, Jerusalem, Israel*

Michael W. Berns, *Department of Developmental and Cell Biology, University of California, Irvine, Irvine, California 92717*

Francis Dumont, *Unité de Cancérologie Expérimentale et de Radiobiologie, INSERM U95, 54500 Vandoeuvre-les-Nancy, France. Present address: Department of Immunology, Merck, Sharp and Dohme Research Laboratories, Rahway, New Jersey 07065*

N. B. Grover, *The Hubert H. Humphrey Centre for Experimental Medicine and Cancer Research, The Hebrew University–Hadassah Medical School, Jerusalem, Israel*

Volker Kachel, *Max-Planck-Institut für Biochemie, D-8033 Martinsried, West Germany*

J. M. Lackie, *Department of Cell Biology, University of Glasgow, Glasgow G12 8QQ, U.K.*

J. Naaman, *The Hubert H. Humphrey Centre for Experimental Medicine and Cancer Research, The Hebrew University–Hadassah Medical School, Jerusalem, Israel*

Gary C. Salzman, *Life Sciences Division, Los Alamos National Laboratory, University of California, Los Alamos, New Mexico 87545*

Robert J. Walter, *Department of Developmental and Cell Biology, University of California, Irvine, Irvine, California 92717*

P. C. Wilkinson, *Department of Bacteriology and Immunology, Western Infirmary, University of Glasgow, Glasgow G11 6NT, U.K.*

Preface

The selective combination of physical, biochemical, and immunological principles, along with new knowledge concerning the biology of cells and advancements in engineering and computer sciences, has made possible the emergence of highly sophisticated and powerful methods for the analysis of cells and their constituents. This series on *Cell Analysis* is, therefore, aiming at providing the theoretical and practical background on how these methods work and what kind of information can be obtained. *Cell Analysis* will cover techniques on cell separation, cell identification and classification, characterization of organized cellular components, functional properties of cells, and cell interactions. Applications in cell biology, immunology, genetics, toxicology, specific diseases, diagnostics and therapeutics, and other areas will be covered whenever relevant results exist.

Nicholas Catsimpoolas
Boston, Massachusetts

此为试读,需要完整PDF请访问: www.ertongbook.com

Contents

Chapter 5

Light Scattering Analysis of Single Cells

Gary C. Salzman

Chapter 6

Methods for Measuring Leukocyte Locomotion

P. C. Wilkinson, J. M. Lackie, and R. B. Allan

Chapter 7

Sizing of Cells by the Electrical Resistance Pulse Technique: Methodology and Application in Cytometric Systems

Volker Kachel

1

Quantification of Red Blood Cell Morphology

JAMES W. BACUS

I. HISTORY

The description of red blood cells extends back to the earliest days of the development of the microscope. In 1658 Swammerdam described the oval red blood cells of the frog, and in 1673 Leeuwenhoek discovered the red cells in human blood and described them as circular in contrast to amphibian cells. In 1770 Hewson published detailed descriptions of structure, form, and dimensions of red blood cells from different animals, including man. In 1846 Gulliver published measurements of red cell size (diameter) on 485 species of vertebrates.

Until this time, descriptions and measurements concentrated on the average diameter of cells from specimens and not on size distributions of cells in individuals. However, by the 1880s various workers had reported red cell diameter sample distributions. During this same period, there was concomitant growth in knowledge and understanding of hemoglobin in red cells. In 1747 Menghini demonstrated the presence of iron in red cells; Funke isolated hemoglobin crystals in 1851; and Hoppe-Seyler had indicated the functional characteristics of oxygen uptake and discharge by 1867. Beginning with the observations of Soret (1878), it was understood that the primary hemoglobin absorption band was in the violet near the visible limit, around 415 nm (Jope, 1949). However, this was largely ignored because of the development of techniques for staining blood by Ehrlich in 1877 (Conn, 1948). The development

JAMES W. BACUS • Medical Automation Research Unit, Rush–Presbyterian–St. Luke's Medical Center, Chicago, Illinois 60612.

此为试读,需要完整PDF请访问: www.ertongbook.com

of these staining techniques stimulated the morphologic study of blood and the relationship between the size and hemoglobin content of the erythrocyte, even though there was no precise stoichiometric relationship between the amount of hemoglobin and the perceived color. In summary, then, by about 1900 the importance of both the size and hemoglobin content of red cells was becoming clear.

From 1880 to 1930, a gradual definition of hypochromic anemia and iron deficiency developed. Lange had first described the disease chlorosis in 1554; by the 1930s this was gradually understood to be iron deficiency anemia as we understand it today (Witts, 1969). Price-Jones (1933) published an exhaustive study of red cell diameter sample distributions for blood from normal individuals and for blood from some individuals with anemia, including iron deficiency. He indicated size changes in both the mean and variances of sample population distributions associated with anemia. Gradually, from the 1920s to the 1940s, the use of the mean red cell size (measured by the hematocrit, divided by the cell count) as proposed by Wintrobe (1930, 1931, 1932, 1934) and others (Jorgensen and Warburg, 1927) became a common measure used to differentiate microcytic anemias from normal. Cooley and Lee (1925) first described thalassemia in the homozygous state. This was later reported in the heterozygous form by Wintrobe *et al.* (1940). Also, Cartwright and Wintrobe (1952, 1966) described the anemia of infection and other chronic disorders in the 1940s and 1950s. Each of these three types of anemia resulted in the production of small hypochromic red cells and thus were potentially confused with each other during differential diagnosis based on changes in mean cell size. The variation in cell size, demonstrated to be important by Price-Jones, was not easily measured and thus was largely ignored as a routine quantitative parameter.

Sorenson (1876) recognized that cells larger than normal were characteristic of pernicious anemias, and Addison (1855) provided the first clinical description of megaloblastic anemia. The description of other macrocytic anemias, e.g., from liver disease and macrocytosis caused by stimulated erythropoiesis, followed this early work. Similarly, other anemias were gradually described by their characteristic red cell morphology. For example, Haden (1934) described measurement relationships between the thickness and diameter of red cells from normal blood and from the blood of patients with spherocytosis. The first morphologic descriptions of the red cells in sickle cell anemia were provided by Herrick (1910).

In many ways, our ability to describe red cells has depended upon the sophistication of our observational and measurement apparatus. The above described development of measurement and quantification of red cells depended upon the development of the microscope, simple counting chambers, hematocrit tubes, and, later, upon advances in chemistry and absorption spec-

troscopy. Ultimately, our current understanding of the disease process and its description have resulted from these measurement capabilities.

In the mid-1900s further advances in microscopy occurred in the area of quantitative microdensitometry. This is probably best characterized by the work of Casperson (1936, 1940), who performed precise microphotometric absorption studies of the nucleic acid of tissue smears. Although this work was limited by current standards with regard to detailed absorption measurements, since the measurement apertures usually encompassed the entire cell or the entire cell nucleus, they provided a clear direction for the potential of quantitative and more automated density and distributional measurements from previously subjective impressions and tedious manual measurement methods. In the 1950s advances in electronics enabled faster scanning with flying spot, television scanning, automatically controlled stage movement and focus, and very small apertures of about 0.15 μm.

In the 1970s several investigators studied red blood cells with variations of these faster, high-resolution scanning methods (Bentley and Lewis, 1975, 1976; Eden, 1973; Green, 1970; James and Goldstein, 1974; Hammarsten *et al.*, 1953). This chapter details studies in our laboratories in this regard (Westerman *et al.*, 1980; Navarro, 1979; Bacus, 1972, 1980; Bacus *et al.*, 1976; Bacus and Weens, 1977). The methods of red cell measurement are described in considerable detail. Then, although the techniques enable, in general, an advanced discriminatory potential when applied to the differential diagnosis of all of the above-mentioned anemias, the hypochromic microcytic anemias are discussed in detail. Through this example it should become clear that just as our current description and understanding of the disease process and our diagnostic ability have resulted from former measurement methods, these new techniques provide additional capabilities for the future.

II. DETAILS OF RED CELL MEASUREMENTS

The specific instrument that we have used in our studies was developed and constructed in our laboratory (Bacus, 1980b). A monolayer blood film preparation is used (Bacus, 1974), and the cells are analyzed microdensitometrically at 415 nm. The cells are not stained prior to analysis. The instrument uses microscope stage motors which move the slide and focus the microscope objective. Conventional microscope optics project cell images on a television scanning imaging sensor. As the microscope stage is moved in a scanning pattern, different red blood cells are located for analysis. Each time the microscope stage stops, all the cells in a given field are measured until a large number of cells has been analyzed.

These techniques have allowed us to make precise detailed measurements

of individual cells. A large number of different measurements has been and can be made since the digitized image of each cell is available for analysis. However, experience has indicated that measurements of hemoglobin content, shape, pallor, and size can be done in a very robust fashion, and these measurements will be discussed in detail below since they form a basis for the quantification of red blood cell morphology by this technology. Other measurements will surely evolve, and, in fact, we have also used additional measurements, but those detailed below form a standard subset.

For the purposes of description, each image may be described as an $n \times n$ measurement matrix, $h(x,y)$, where each value of $h(x,y)$ is a measured point of absorbance obeying the Beer–Lambert absorption law:

$$h(x,y) = \log \frac{I_0}{I_t} = \frac{\mathbf{km}}{\mathbf{a}} \tag{1}$$

where I_0 is the incident light, I_t is the transmitted light, k is the specific absorptivity of hemoglobin under these conditions, m is the mass of hemoglobin for that picture element measurement point, and a is the measurement spot size.

A convenient way to locate objects, i.e., red blood cells, for measurement is to set a clipping level at a low absorbance and to make measurements on objects that are above this clipping level. Thus for a single red blood cell in a field of view,

$$H = \frac{a}{k} \sum_x \sum_y h(x,y) \tag{2}$$

results in a measurement of the mass of hemoglobin (H) for that cell.

The cell area (A) and the boundary perimeter (P) are computed from an octal chain code representation of the outer cell boundary. The octal chain code is determined by searching around the clipping threshold level to outline the cell of interest. Generalized techniques of octal chain code analysis have been described by Freeman (1974), and some of the included descriptions follow his notation. Each chain code element is indicated by a_i, $i = 1,2,3, \ldots, n$. Each a_i is an integer from 0 to 7. Also, each element has a length of 1 for even a_i and $\sqrt{2}$ for odd a_i. Thus the perimeter (P) of an object, with N_e the total number of even valued elements and N_o the total number of odd elements, is:

$$P = N_e + N_o \times \sqrt{2} \tag{3}$$

The following relationship exists between the x,y coordinate system, or the digitized grid, and the elements a_i of the chain.

a_i	a_{ix}	a_{iy}
0	1	0
1	1	1
2	0	1
3	−1	1
4	−1	0
5	−1	−1
6	0	−1
7	1	−1

(4)

Given the initial y value, Y_0, this relationship is used according to equation (3) to find the area (A) enclosed by the chain code.

$$A = \left| \sum_{i=1}^{n} a_{ix}(Y_{i-1} + \tfrac{1}{2}a_{iy}) \right| \tag{5}$$

A robust measurement of shape, which is particularly applicable to red cells, comes from a theorem in the real plane known as the isoperimetric inequality (Courant and Hilbert, 1937; Polya and Szego, 1951). This states that the perimeter squared divided by the area is greater than or equal to 4π, with equality holding if and only if the perimeter is in the shape of a circle. If two shapes are geometrically similar, i.e., they have the same shape but different sizes, they will have the same p^2/A since the perimeter increases linearly with the size, while the area increases with the square of the size. However, a multiplicity of different shapes may result in the same p^2/A greater than 4π. Thus, for digital red blood cell images, p^2/A is a convenient measure of circularity; however, because of the digital nature of the image, the boundaries of the image are represented as a polygon. Examples of area and circularity measurement results are shown for three octal chain coded line drawings of the closed contours in Fig. 1. Table I details the feature calculation for the contour of Figure 1a. Table I is arranged such that the calculated value of equation (5), for each summation step, is in the left column. The information relevant to the calculation is in the next five columns, in the same row. For example, the octal chain code for each contour is in column 3.

Of course, a circle cannot be represented exactly on a course grid. Figure 2 indicates circular polygons of the best fitting circles to a grid with different radius values. It turns out that, depending on the placement of an object on the sampling grid, an error will result in the p^2/A measure which is a function of the fineness of the digital resolution. Figure 3 is a graph of p^2/A as a function of the radius of digitally generated round objects. For circular polygons the

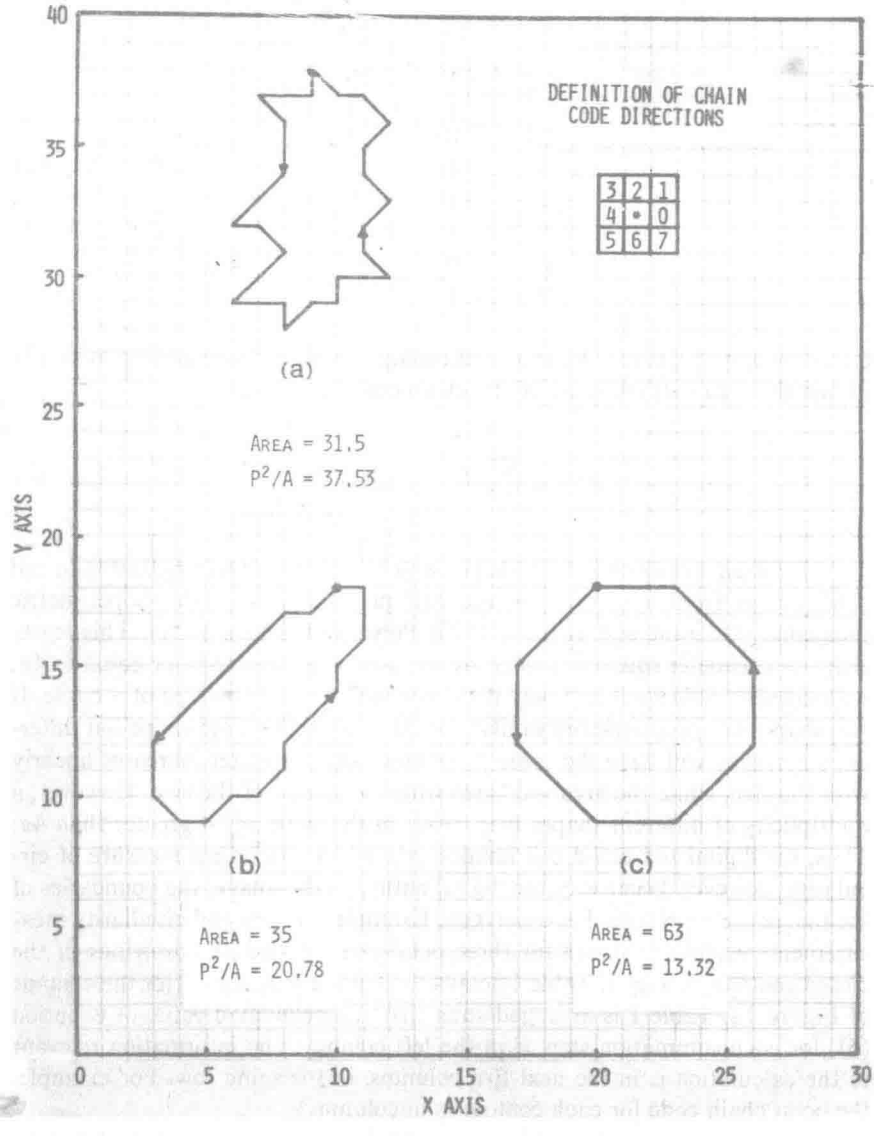

FIGURE 1. Three closed contour octal chain coded boundary shapes, similar to red cell outlines. Area and p^2/A have been computed for each of the boundaries. Detailed computations for (a) are in Table I. The arrow indicates the direction of boundary tracing to form the chain code from •, the initial x,y coordinate starting point.

TABLE I
Method of Calculating Area and p^2/A from Octal Chain Code of Closed Contour of Figure 1a

$a_{ix}(Y_{i-1} + \frac{1}{2}a_{iy})$	i	a_i	Y_{i-1}	a_{ix}	a_{iy}
0	1	6	38	0	−1
−37	2	4	37	−1	0
−37	3	4	37	−1	0
37	4	7	37	1	−1
0	5	6	36	0	−1
0	6	6	35	0	−1
−33.5	7	5	34	−1	−1
−32.5	8	5	33	−1	−1
32	9	0	32	1	0
31.5	10	7	32	1	−1
−30.5	11	5	31	−1	−1
−29.5	12	5	30	−1	−1
29	13	0	29	1	0
29	14	0	29	1	0
0	15	6	29	0	−1
28.5	16	1	28	1	1
29	17	0	29	1	0
0	18	2	29	0	1
30	19	0	30	1	0
30	20	0	30	1	0
−30.5	21	3	30	−1	1
0	22	2	31	0	1
32.5	23	1	32	1	1
−33.5	24	3	33	−1	1
0	25	2	34	0	1
35.5	26	1	35	1	1
−36.5	27	3	36	−1	1
−37	28	4	37	−1	0
−37.5	29	3	37	−1	1
$\lvert\Sigma\rvert = 31.5$	Area = 31.5		$P = 16 + 13\sqrt{2} = 34.38$		
	$p^2/A = 37.53$				

limiting value is approximately 13.9810 (Navarro, 1979). It can also be proven that p^2/A has a lower bound of 13.25484, which is the lowest digitized value that can possibly be achieved (Navarro, 1979).

One of the more important morphologic features of mammalian red blood cells is their "central pallor." Typically, this is a round, central, biconcave area of decreased thickness, resulting in a decreased central absorbance. The hypochromic red cell is described as a cell with an exaggeration of normal central pallor (Bacus, 1980a). Our quantitative definition of central pallor uses the

此为试读,需要完整PDF请访问: www.ertongbook.com